Thermochimica Acta, 54 (1982) 35–45
Elsevier Scientific Publishing Company, Amsterdam—Printed in The Netherlands

TRANSPORT PROPERTIES OF MOLYBDENUM TRIOXIDE AND ITS SUBOXIDES

M.A. KHILLA, Z.M. HANAFI, B.S. FARAG and A. ABU-EL SAUD

National Research Centre, Dokki, Cairo (Egypt)

(Received 2 September 1981)

ABSTRACT

The electrical conductivity σ_{AC} and thermoelectric power α for the MoO_3–MoO_{3-x}–MoO_2 system, namely MoO_3, $Mo_{13}O_{38}$, Mo_9O_{26}, Mo_8O_{23}, $Mo_{17}O_{47}$, Mo_4O_{11} and MoO_2, are measured over a wide temperature range. The conductivity value at room temperature is found to increase with departure from stoichiometry. MoO_3 and its suboxides exhibit semiconducting behaviour while MoO_2 at low temperature exhibits semimetal-like character of $10^{-2}\ \Omega^{-1}\ cm^{-1}$ rather than a semiconducting one. Above room temperature MoO_2 gave a ΔE value of 0.85 eV, indicating that this metal-like conduction is not taking place. Some discontinuities are present in the $\log \sigma$ vs. $1/T$ curves for all samples. These are confirmed by DTA.

The thermoelectric power indicates that all oxides are *n*-type semiconductors up to 300°C. The value at room temperature decreases with departure from stoichiometry. The most pronounced change of both σ and α is at Mo_8O_{23}, i.e. at $x=0.125$.

INTRODUCTION

It is well known that MoO_3 forms a series of suboxides. The existence of several phases in the MoO_3–MoO_2 system had been revealed by Kihlborg [1] and Magnéli [2]. Their crystal structure and formulae were well established. The electrical conductivity of MoO_3 was previously measured on single crystal [3–12] and polycrystalline samples [8–10,13–22]. It was also measured on the melt [23]. The conductivity varied from $10^{-15}\ \Omega^{-1}\ cm^{-1}$ at −70°C [3] for a single crystal and from $10^{-8}\ \Omega^{-1}\ cm^{-1}$ at 20°C to $10^{-3}\ \Omega^{-1}\ cm^{-1}$ at 350°C for polycrystalline MoO_3 [13]. The resistivity decreased from 10^5 to 30–40 Ω on melting. The activation energy varied from 0.5–0.2 eV [3] and 0.87–1.12 eV [4] for single crystals and 0.56 eV for polycrystalline MoO_3 [19]. The decrease in conductivity with an increase in oxygen pressure indicated *n*-type conduction [8,20]

The electrical conductivity of MoO_2 was measured at high temperature by Friederich and Sittig [24]. Pekar [25] found a new conception of the electronic conductivity of ionic crystals of MoO_2. This concept gave theoretical calculation for mobility which coincided with the experimental data of conductivity and Hall constant. Vickery and Hipp [26] measured the conductivity of MoO_2 single crystal which was *n*-type and as low as $0.5\ \Omega^{-1}\ cm^{-1}$.

Few authors have dealt with the measurement of the thermoelectric power of MoO_3 [10,27]. Differential thermal analysis was studied by Trambouza et al. [28]. It was found that MoO_3 undergoes an endothermic transition between 350 and 500°C. There was no change in chemical composition as measured by weight change. The transformation is reversible but X-ray and IR absorption measurements show no change accompanying this transition. Only a break in the density temperature curve is observed at about 400°C.

Very little information is available about the variation of the transport properties of this system with variation of the O:Mo ratio. The aim of this work is to trace the variation of σ and α with the departure of the O: Mo ratio. This is a continuation of previous similar studies carried out on the magnetic susceptibility [29], IR absorption [30] and diffuse reflectance [31].

EXPERIMENTAL

Samples included in this study are MoO_3, $Mo_{13}O_{38}$, Mo_9O_{26}, Mo_8O_{23}, $Mo_{17}O_{47}$, Mo_4O_{11} and MoO_2. The starting materials for preparation were MoO_3 (Merk) heated in a stream of oxygen at 600°C and spec pure Mo metal (Johnson and Matthey, England), powdered and heated in vacuum at 400°C. The samples were prepared according to Magnéli [2] by thoroughly mixing weighed amounts of Mo and MoO_3. These mixtures were heated at the appropriate temperature in evacuated silica tubes as previously described [30].

The conductivity measurements were carried out using a simple circuit by the application of Ohm's law as reported previously [32]. The thermoelectric power was measured according to the method of Middleton and Scaolon [33].

Differential thermal analysis was carried out using type Linseis (Selb, F.R.G.).

RESULTS AND DISCUSSION

The electrical conductivity σ_{AC} was measured over the temperature range −190 to 500°C for MoO_3 and up to 300°C for the different suboxides. Figures 1 and 2 represent the course of the conductivity variation against the reciprocal of temperature. As can be seen, all curves reveal an approximately horizontal region extending from −190 up to 0°C. This is due to the frozen-in impurities, where the defects are less mobile and most of the carriers are frozen on cations. This is the case with MoO_3 and the samples with low oxygen deficiency, namely $Mo_{13}O_{38}$, Mo_9O_{26} and Mo_8O_{23}, while $Mo_{17}O_{47}$ and Mo_4O_{11} show semimetal-like character which increases relatively with decrease of oxygen: metal ratio.

This metal-like character can be seen clearly in Fig. 2 with MoO_2 which exhibits a high electrical conductivity value of $10^{-2}\ \Omega^{-1}\ cm^{-1}$ with temperature dependence. This result is in agreement with the finding of Perloff and Wold [34] and Rogers et al. [35]. Rogers pointed out that the short interaction separation within metal atom

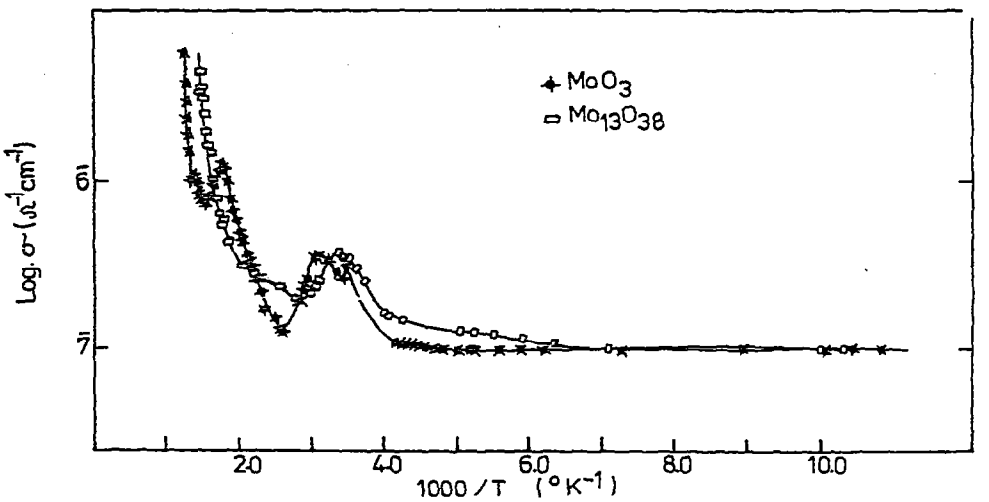

Fig. 1. Variation of log electrical conductivity with the reciprocal of the absolute temperature for MoO_3 and $Mo_{13}O_{38}$.

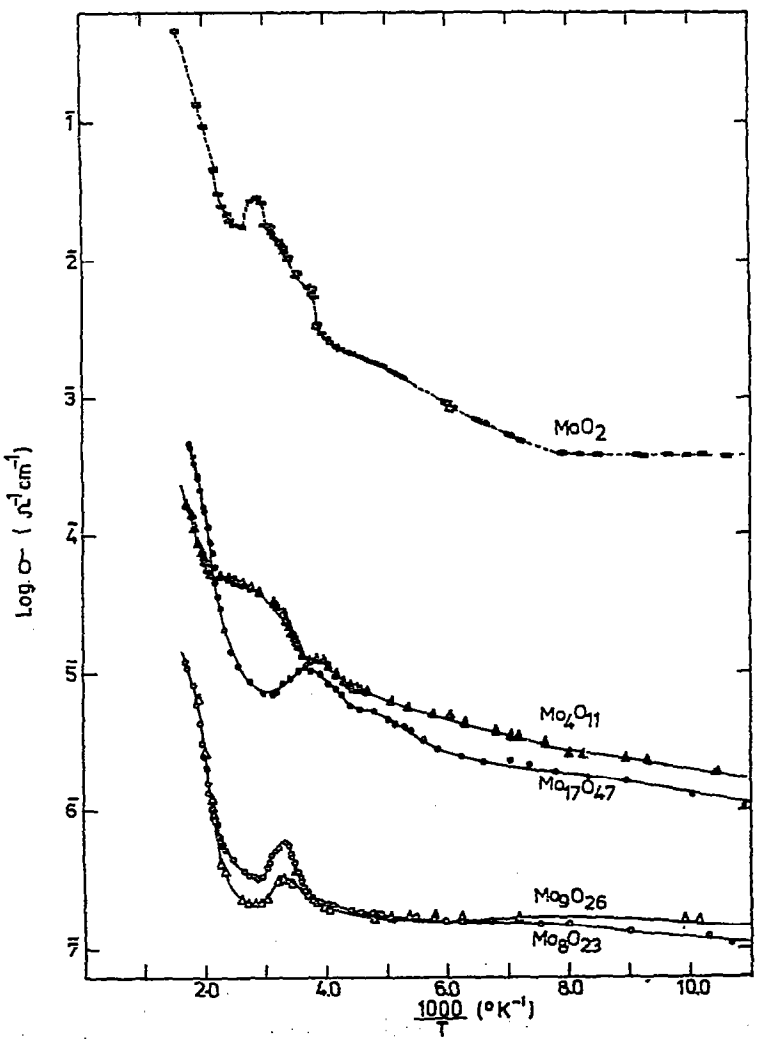

Fig. 2. Variation of log electrical conductivity with the reciprocal of the absolute temperature for MoO_2, Mo_4O_{11}, $Mo_{17}O_{47}$, Mo_9O_{26} and Mo_8O_{23}.

doublets in this oxide structure (distorted rutile) indicates the presence of strong metal–metal bonding and a close relationship exists between the axial ratios of this oxide and the number of free valence electrons available per bond. Goodenough [36] argued that metallic conductivity may arise either by direct overlap of *d*-wave functions or by strong covalent mixing of cationic and ionic *s* and *p* wave functions. Applying this model to rutile related structures, it was found that MoO_2 not only has

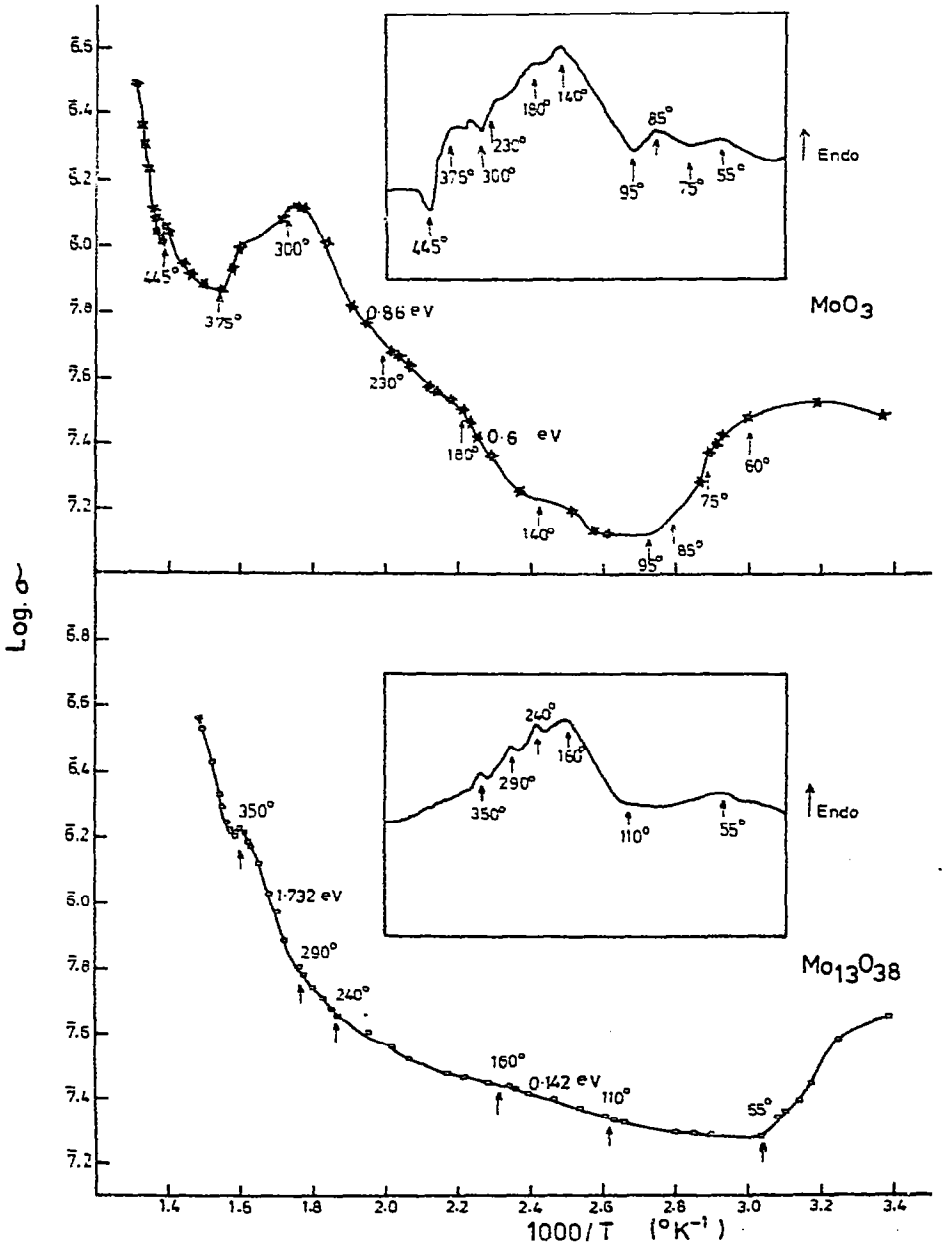

Fig. 3. DTA curve and variation of log electrical conductivity with the reciprocal of the absolute temperature for MoO_3 and $Mo_{13}O_{38}$.

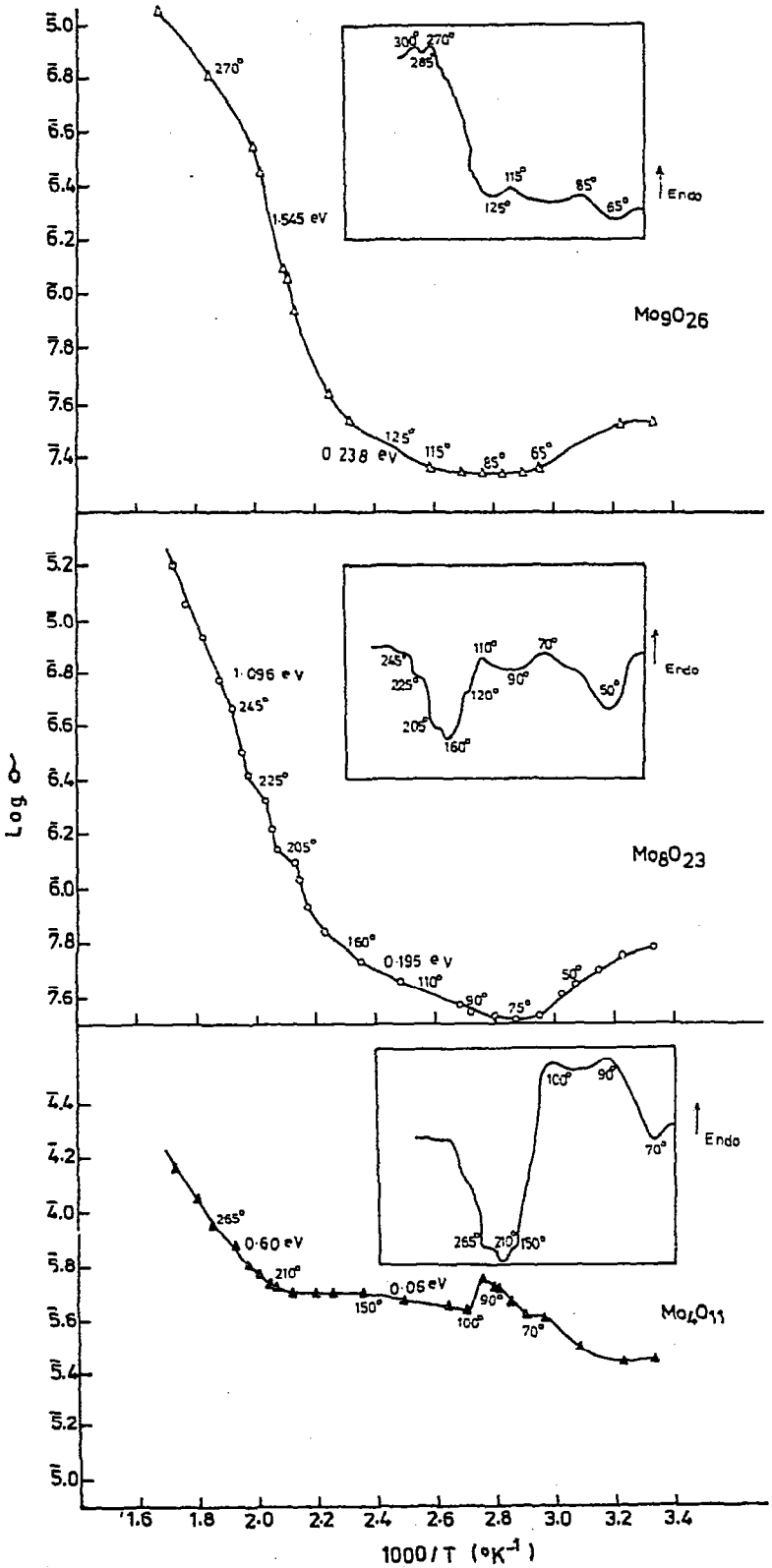

Fig. 4. DTA curve and variation of log electrical conductivity with the reciprocal of the absolute temperature for Mo_9O_{26}, Mo_8O_{23} and Mo_4O_{11}.

one electron available for metal bonding but also has one π^* electron to partially fill the π^* band. Hence this accounted for the occurrence of both the cationic doublets and metallic conductivity in MoO_2.

Indeed MoO_2 has a conductivity with a metallic temperature coefficient in the region of room temperature, in agreement with Morin [37].

As the temperature rises, carrier concentration results in a low change of conductivity for all samples. Above a certain temperature the increase becomes rapid and the behaviour is that of typical semiconductors. Some peaks and valleys are detected through plots of $\log\sigma$ vs. $1/T$, which vary from sample to sample. These plots are clearly manifested in Figs. 3–6, together with the corresponding differential thermal analysis curves. These Figs. are classified according to the structural families of the compounds [1].

Considering Fig. 3 representing the behaviour of the MoO_3 family, it is clear that MoO_3 exhibits a maximum at 50–60°C and then drops to a minimum value at about 100°C. This maximum completely disappeared when the experiment was repeated on a sample previously heated to 100°C under vacuum of 10^{-3} mm Hg for 1 h, which confirms that this may be due to the presence of OH^- groups as stated by Ioffe et al. [10]. A similar dehydration reaction with its peak in the temperature range 55–100°C is traced on the DTA curves. This endothermic reaction is attributed to the loss of interlayer and surface adsorbed water present.

After 100°C the conductivity increases with temperature and the relation $\sigma = \sigma_0 \exp -\Delta E/2kT$ is applicable in certain ranges with maxima and interruptions of the linear relation at 140, 180, 230, 300, 375 and 445°C in the case of MoO_3. A full discussion of its electrical conductivity has been published [38].

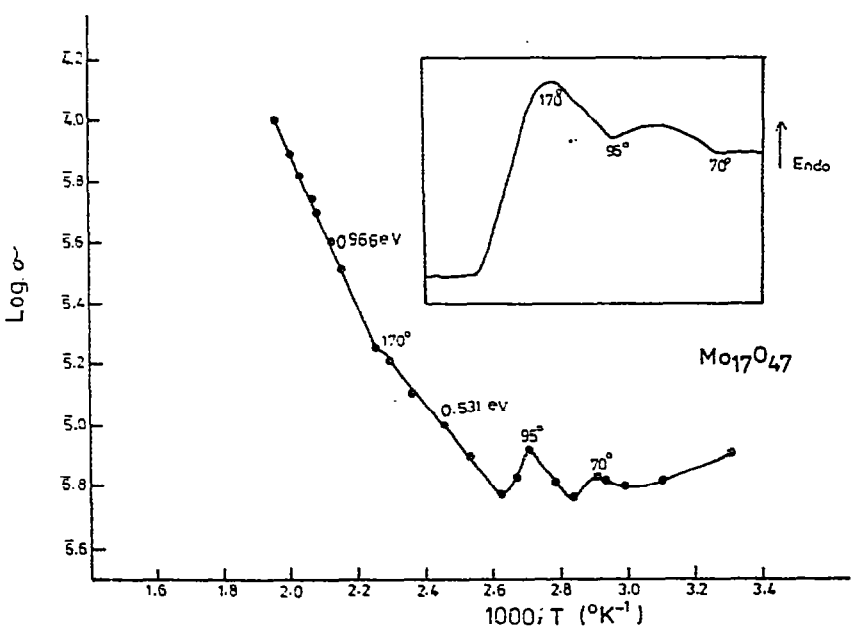

Fig. 5. DTA curve and variation of log electrical conductivity with the reciprocal of the absolute temperature for $Mo_{17}O_{47}$.

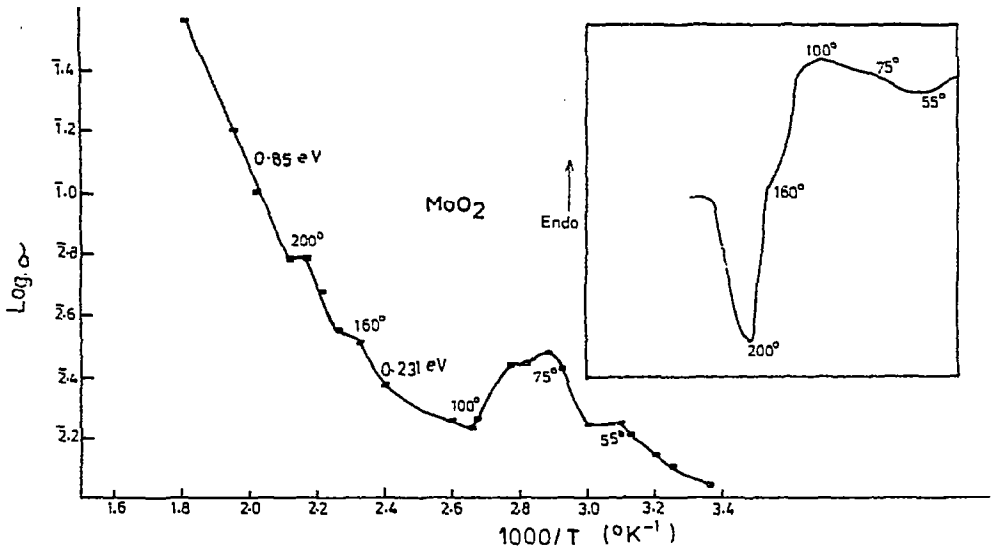

Fig. 6. DTA curve and variation of log electrical conductivity with the reciprocal of the absolute temperature for MoO_2.

The temperature dependence of σ for MoO_2 above room temperature is plotted in Fig. 6. The σ value increases with temperature and possesses discontinuities in the range 55--100°C and 200°C. The first may be due to water molecules adsorbed on the surface of the sample. The second, at 200°C, may be due to a change in the carrier mobility arising from either (i) a change in the scattering mechanism, (ii) an increase in the effective mass, or a combination of both. Alternatively, this may be due to (iii) phase change from one crystallographic modification to another leading to a change in the electronic structure [39]. The absence of X-ray proof at high temperatures leads to its confirmation by DTA alone, where the changes in the EMF and σ are found to occur in the same temperature regions.

The application of the above-mentioned relation of σ and $1/T$ led to ΔE values of 0.231 and 0.85 eV, respectively. Chase [40] observed a peak at 0.8 eV in the optical conductivity and it was taken as evidence that normal metallic conduction is not occurring, as is the case in the low temperature range.

The variation of the electrical conductivity for the samples between MoO_3 and MoO_2 is represented in Figs. 3–5 with the corresponding DTA curves. The behaviour of the suboxides above room temperature is typically semiconducting. The value of σ increases with rise in temperature but still preserves the discontinuities observed in the case of MoO_3 and MoO_2. This behaviour varies from sample to sample. If these are compared within each family, it is noticed that MoO_3 and $Mo_{13}O_{38}$ behave similarly. This may be due to the fact that the variation in the number of free electrons and the effective mass is very small [29].

The ReO_3 family members Mo_9O_{26} and Mo_8O_{23} behave similarly. This may be due to the fact that their crystal structures are closely interrelated and differ only in the width of the slab. Mo_4O_{11} of the ReO_3 family shows a behaviour which is deviated more towards that of $Mo_{17}O_{47}$ of the mixed polygonal network structure of

the order of $10^{-5}\ \Omega^{-1}\ cm^{-1}$. Mo_4O_{11} is somewhat different to Mo_9O_{26} and Mo_8O_{23} from the structural point of view. The orientation of this suboxide relative to the slab is quite different. A further difference is found in the mutual connection of the slabs. In Mo_4O_{11}, these slabs are not condensed upon each other but mutually connected by MoO_4 tetrahedra which share three corners with two octahedra in one slab and the remaining corners with an octahedron in the next slab [1]. The difference between the different suboxides may be due to their different family structures [30].

Differential thermal analysis

As shown above, the curves recorded by DTA indicate not only the thermal effects related to dehydration (in the range room temperature to about 120°C) but also the physical changes which the molybdenum oxide series (MoO_3–MoO_{3-x} – MoO_2) undergo as a result of thermal energy. A dehydration reaction, with its peak in the temperature range 50–100°C, is traced on all curves of molybdenum oxides.

For MoO_3 and $Mo_{13}O_{38}$ samples an endothermic effect occurs at about 140–160°C, 230–240°C and 350–370°C. These are assigned to the transfer of oxygen mobility from a lower to a higher level in the crystal lattices of these oxides. The exothermic changes in the MoO_3 curve at 300 and 445°C can be attributed to either recrystallization of MoO_3 or to the transfer of MoO_3 crystals to a well-defined type. It is clear from the DTA of MoO_3 that this process started at 375°C and reached its maximum at 445°C. The small endothermic change in the $Mo_{13}O_{38}$ curve at 290°C is also attributed to the change in oxygen mobility in the crystal.

It is well known that there is a characteristic temperature for each compound, depending on the nature of the crystalline structure, at which the atoms or groups of atoms obtain the necessary mobility for changing their position. At these temperatures thermal agitation begins to manifest itself first by a vibration of the atoms at the points which they occupy in the lattice. By further raising the temperature the vibrations of the atoms are amplified, and thus a change in their position becomes possible. This may explain the movement of oxygen atoms in the lattices of MoO_3 and $Mo_{13}O_{38}$ with the appearance of the endothermic changes obtained [28].

Over the whole temperature range used in the DTA of MoO_3 and $Mo_{13}O_{38}$, as well as in all the molybdenum oxide series, the base line always deviates more or less from a straight line. This may be attributed firstly as a result of a change in the physical properties of the tested samples due to the thermal changes which has taken place; secondly, it may also be produced due to the inequality of heat conductivity and specific heat of molybdenum oxides and those of the thermally inert Al_2O_3. So it is clear that the DTA characteristics of MoO_3 and $Mo_{13}O_{38}$ are very similar since they are related to the same MoO_3 family.

Observing the second family which contains Mo_9O_{26}, Mo_8O_{23} and Mo_4O_{11}, the following conclusions are drawn from the DTA curves.

(1) In the Mo_9O_{26} sample the DTA characteristics give endothermic changes at 270–285°C and at 300°C which are attributed to the increase in oxygen mobility in the crystal lattice of this oxide.

(2) With respect to Mo_8O_{23}, the thermal change begins to reverse its sign up to 110°C to give an exothermic change at 160°C. Small exothermic effects at 205, 225 and 245°C are obtained, which may be attributed to the recrystallization characteristics of this oxide.

(3) The same behaviour of Mo_8O_{23} is also observed in the case of Mo_4O_{11} but with respect to Mo_4O_{11} the first exothermic change occurs at 150°C and the small exothermic effects at 210 and 265°C.

The disappearance of the endothermic changes and the reversing of the sign of the DTA curves obtained for Mo_8O_{23} may be attributed to the fact that with decreasing the oxygen in the lattice, the oxide formed to reach its neutrality in charge must represent

(a) increase in oxygen valency for the oxygen atoms in the cystal lattice, which leads to the increase of electronegativity of the oxygen;

(b) Distortion of the MoO_6 octahedron which can be regarded as a displacement towards the slab boundaries of the oxygen lattice relative to the metal lattice [1];

(c) decrease in the average valency of molybdenum in the oxide crystal lattice.

These three factors cause increased capture of oxygen in the lattice and decreased oxygen mobility. Furthermore, it reverses the sign of the thermal change to exothermic. This is further proved by the increase of the exothermic peak in the case of Mo_4O_{11} and MoO_2, with the decrease of oxygen in the lattices.

The observed results of $Mo_{17}O_{47}$ are not coincident with the latter explanation. This is due to the fact that $Mo_{17}O_{47}$ gives an endothermic change, first at 70–95°C which is attributed to the first dehydration step, and then the second dehydration step begins at 95°C to cover the exothermic change which is found to start at 170°C instead of 150°C in the case of Mo_4O_{11} and at 160°C in case of Mo_8O_{23}. So these two exothermic changes which occurred in these two latter oxides disappeared in the DTA curves of $Mo_{17}O_{47}$. This may be due to the mixed polygonal network structure.

As far as the authors are aware, there is no mention in the literature concerning either the phase changes or the effect of temperature on this series of oxides. The only available study is that of Deb and Chopoorian [19] where no significant change could be found in the line intensity of the X-ray diffraction pattern in the temperature range 25–500°C that could be indicative of a polymorphic phase change. This needs further confirmation using a high temperature X-ray camera.

Thermoelectric power

The thermoelectric power α was measured in the temperature range 20–300°C. The sign of α was negative for all samples. The general behaviour of the thermoelectric power decreases on going from 20 to 300°C, except in the case of $Mo_{17}O_{47}$ and Mo_4O_{11} where α decreases then increases again and becomes approximately constant.

The room temperature values of α for the different oxides are illustrated in Fig. 7. It is clear that there is a sharp decrease in the thermoelectric power value after the composition Mo_8O_{23}, i.e. at $x = 0.125$. This is also clear in the variation of σ values

at room temperature. The conductivity increases with increase of oxygen deficiency, also with the pronounced variation after Mo_8O_{23} composition. From all other properties previously measured, it is clear that Mo_8O_{23} divides this O: Mo range into two regions at $x = 0.125$.

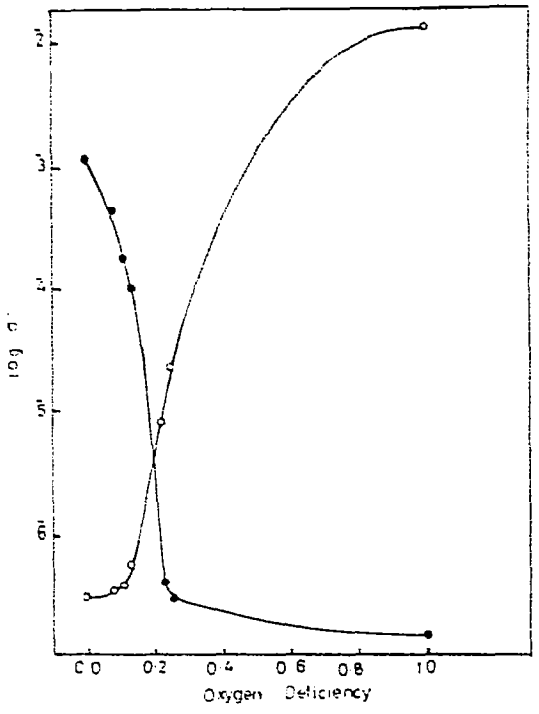

Fig. 7. Variation of log electrical conductivity (○) and the thermoelectric power (●) with oxygen deficiency at room temperature.

The present representation of σ and α with O:Mo ratio indicates that the type of current carriers is the same throughout this composition range, i.e. *n*-type electronic semiconductors.

REFERENCES

1 L. Kihlborg, Ark. Kem., 21 (1963) 471.
2 A. Magnéli, Acta Chem. Scand., 9 (1955) 1478
3 P. Stahelin and G. Busch, Helv. Phys. Acta, 23 (1950) 530.
4 N.M. Gvilova, E.Z. Nemsadze and Z.N. Chigogidze, Tr. Tbiliss. Gos. Univ., 86 (1960) 459.
5 A.L. Shkol'nik, Soobshch. Akad. Nauk Gruz. S.S.R., 47 (3) (1967) 551.
6 A.L. Shkol'nik, Izv. Akad. Nauk S.S.S.R. Ser. Fiz., 31 (1967) 2050.
7 J. Pluta, Z. Phys. Chem. (Frankfurt), 58 (1–4) (1968) 189.
8 A.K. Ishkneli, M.G. Onikashvili and A.L. Shkol'nik, Soobshch Akad. Nauk Gruz. S.S.R., 53 (1969) 61.
9 S.K. Deb, Proc. R. Soc. London, Ser. A, 404 (1477) (1968) 215.
10 V.A. Ioffe, I.B. Patrina, E.V. Zeienetskaya and V.P. Mikheeva, Phys. Status Solidi, 35(1) (1969) 535.
11 W.G. Buckman, J. Appl. Phys., 43(2) (1972) 1280.

12 K. Teges, Mag. Fiz. Foly., 23(3) (1975) 195.
13 L. Sacconi and R. Cini, J. Chem. Phys., 18 (1950) 1124.
14 V.P. Elyutin, Yu.A. Pavlov, Yu.N. Surovoi and V.I. Shulepov, Izv. Vyssh. Uchebn. Zaved., Chern. Metall., 7 (1961) 12.
15 V.P. Elyutin, Yu.A. Pavlov and Fu. K'ang Ts'ao, Izv. Vyssh. Uchebn. Zaved. Chern. Metall., 5(1) (1962) 14.
16 V.P. Elyutin, Yu.A. Pavlov, V.I. Shulepov and T.G. Myakisheva, Zh. Fiz. Kim., 36 (1962) 1524.
17 S. Minomura and H.G. Drickamer, J. Appl. Phys., 34 (10) (1963) 3040.
18 A.M. Liquori and B. Pispisa, Ric. Sci., Parte 2, Sez. A, 6 (1964) 653.
19 S.K. Deb and J.A. Chopoorian, J. Appl. Phys., 37 (13) (1966) 4818.
20 A.K. Ishkneli, M.G. Onikashvili and A.L. Shkol'nik, Izv. Vyssh. Uchebn. Zaved. Fiz., 12 (1969) 131.
21 G.S. Nadkarni and T.G. Simmons, J. Appl. Phys., 43(2) (1972) 3741.
22 Yu. A. Pavlov, V.B. Polyakov and V.V. Ploshkin, Izv. Vyssh. Uchebn. Zaved. Chern. Metall., 11 (1974) 9.
23 A.E. Van Arkel, E.A. Flood and N.F.H. Bright, Can. J. Chem., 31 (1953) 1009.
24 E. Friederich and L. Sittig, Z. Anorg. Chem., 145 (1925) 137.
25 S.I. Pekar, J. Appl. Phys. U.S.S.R., 18 (1948) 105.
26 R.C. Vickery and J. Hipp, J. Appl. Phys., 37(7) (1966) 2926.
27 I.N. Plaksin, Yu.N. Matveev, B.Ya. Platavtsev and L.N. Storozhev, Dokl. Akad. Nauk S.S.R., 195(1) (1967) 140.
28 Y. Tranibouza, Y. Colleuille and Tran Hun The, C.R., 242 (1956) 497.
29 M.A. Khilla, H. Mikhail, Abu-El Saud and Z. M. Hanafi, Czech. J. Phys., B30/9 (1980) 1039.
30 Z.M. Hanafi, M.A. Khilla and A. Abu-El Saud, Rev. Chim. Mineral., 12 (1975) 546.
31 Z.M. Hanafi, M.A. Khilla, and A. Abu-El Saud, Rev. Chim. Mineral., 18 (1981) 133.
32 A.R. Tourky, Z.M. Hanafi and K. El-Zewel, Z. Phys. Chem., 242 (1969) 298.
33 A.E. Middleton and W.W. Scaolon, Phys. Rev., 92 (1953) 219.
34 D.S. Perloff and A. Wold, in H.S. Peiser (Ed.), Crystal Growth, Proc. Int. Conf. Crystal Growth Pergamon Press London, 1967.
35 D.B. Rogers, R.D. Shannon, A.W. Slight and J.L. Gilson, Inorg. Chem., 8(4) (1969) 841.
36 J.B. Goodenough, Bull. Soc. Chim. Fr., 4 (1965) 1200.
37 F.J. Morin, J. Appl. Phys. Suppl., 32 (1961) 4195.
38 M.A. Khilla and A.A. Hanna, Bull. NRC, Egypt, 1 (1976) 16.
39 Z.M. Hanafi and M.A. Khilla, Z. Phys. Chem. N. F., 82 (1972) 209.
40 L.L. Chase, Phys. Rev. B, 10(6) (1974) 2226.